Supporting information for

Two pairs of chiral Yb^{III} enantiomers presenting distinct NIR luminescence and circularly polarized luminescence performances with giant differences in second-harmonic generation responses

Xiaodi Du,*[a] Zhiqiang Zhang,[b] Congli Gao,[b] Fengcai Li,[b] and Xi-Li Li*[b]

[a]*College of Chemistry and Chemical Engineering, Zhoukou Normal University, Zhoukou 466001, China. E-mail: duxiaodi2000@163.com*

[b]*Henan Provincial Key Laboratory of Surface and Interface Science, Zhengzhou University of Light Industry, Zhengzhou 450002, China. E-mail: lixl@zzuli.edu.cn*

Table of Contents

Measurement details:

1. CPL measurement:

Solid-state CPL spectra of **D-1**/**L-1** and **D-2**/**L-2** were record on an OLIS NIR-CPL SOLO based on their crystalline samples which were ground and then well-sandwiched by using two quartz slides. In addition, to eliminate the potential contributions of linear dichroism and birefringence, different spectra were recorded by rotating each sample by ±45° and ±90° around the optical axis, and by flipping each sample by 180° around the axis perpendicular to the light beam. The average spectra were adopted and reported.

2. Characterization technique for nonlinear optical (NLO) response:

Schematic diagram of the device for testing NLO responses of crystalline materials has been reported elsewhere.[1] Excitation light (λ_{ex} = 1550 nm) is generated by using an ultrafast fiber laser (100 mW, NPI Lasers, Rainbow 1550 OEM), whose pulse width is 100 fs and the repetition rate is 80 MHz. Then the light beam is focused by using an aspheric lens (N.A. = 0.8) to form a laser spot on the crystalline sample with the beam waist radius being 2 μm. The measurements of SHG responses for **D-1**/**L-1**, **D-2**/**L-2**, $Yb(btfa)_3(H_2O)_2$, $Yb(dbm)_3(H_2O)$ and KDP were conducted using their crystalline samples with the identical particle size range (< 30 μm). Their SHG signals were obtained under the identical integration time (T_{int} = 0.5 s), and their SHG spectra are recorded on a cooled fiber optic spectrometer (Ideaoptics, NOVA).

Reference:

1. M. Cui, L. Yang, F. Li, L. Zhou, Y. Song, S.-M. Fang, C.-M. Liu and X.-L. Li, *Inorg. Chem*., 2021, **60**, 13366–13375.

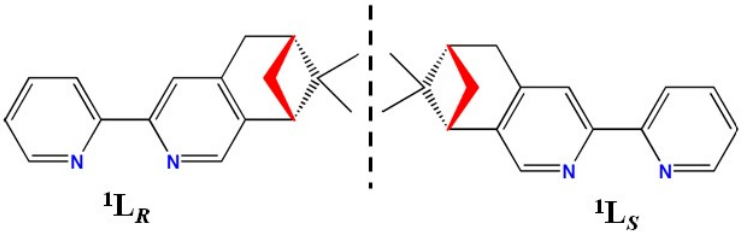

Scheme S1. Chemical structures of enantiomerically pure bidentate *N*-donor ligands ^1L_R/^1L_S.

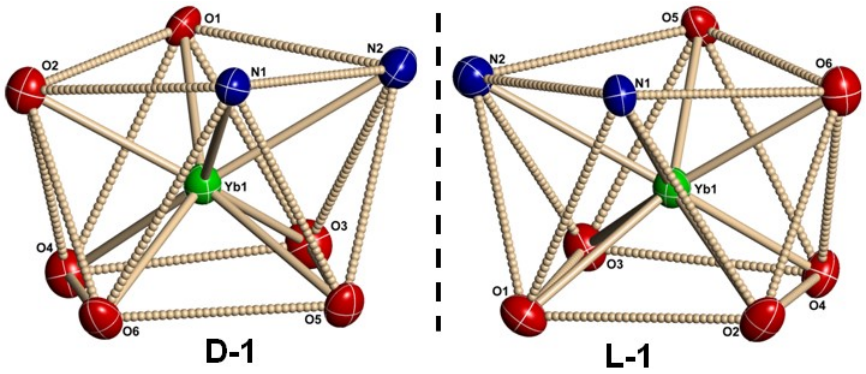

Fig. S1. Coordination geometries of Yb1 in **D-1** and **L-1**.

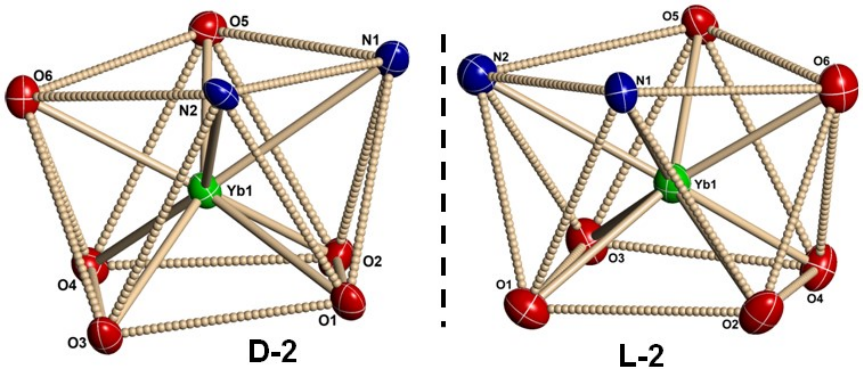

Fig. S2. Coordination geometries of Yb1 in **D-2** and **L-2**.

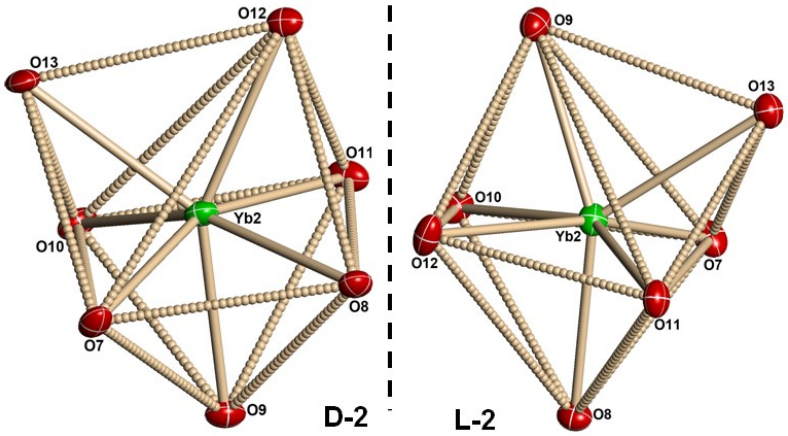

Fig. S3. Coordination geometries of Yb2 in **D-2** and **L-2**.

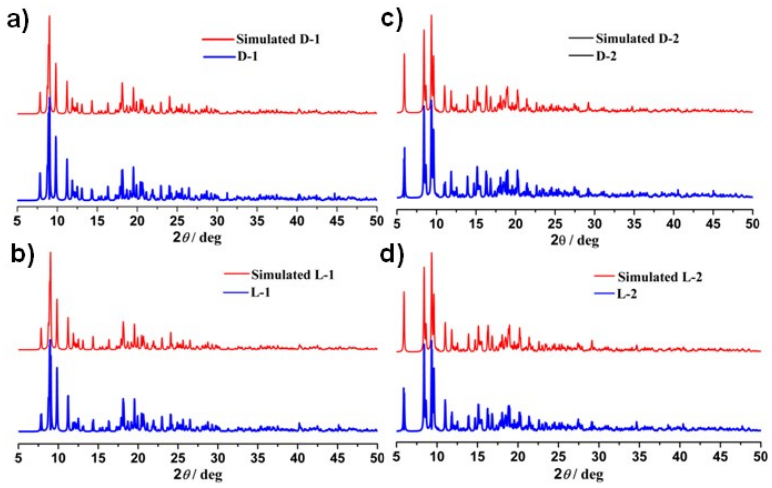

Fig. S4. Simulative and experimental PXRD patterns for **D-1**/**L-1** (a/b) and **D-2**/**L-2** (c/d).

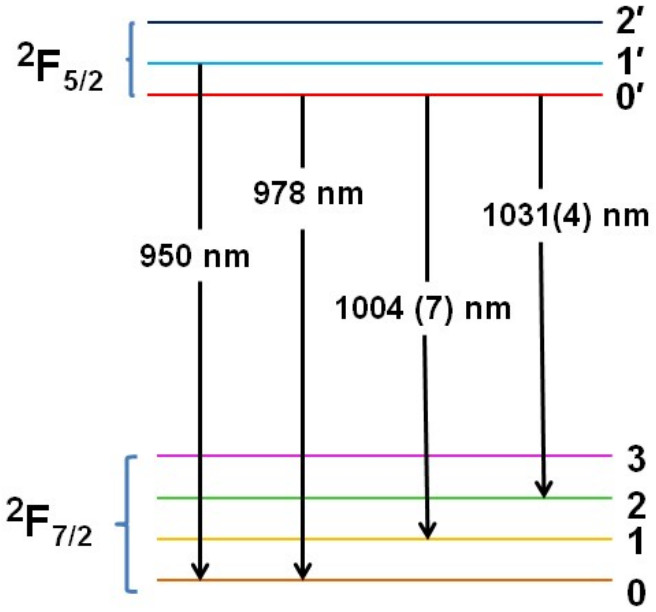

Fig. S5. Energy levels corresponding to the Yb^{III} emissions in **D-1** and **D-2**.

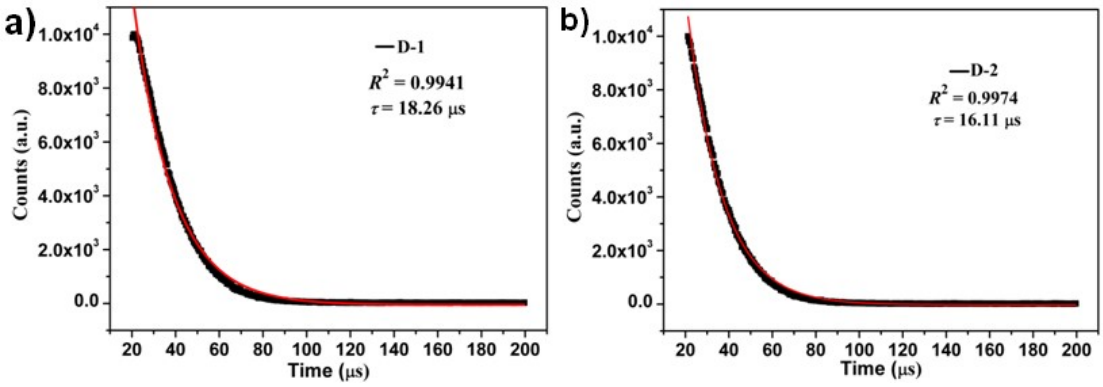

Fig. S6. Solid-state decay curves of **D-1** (a) and **D-2** (b) with fitted curves (red).

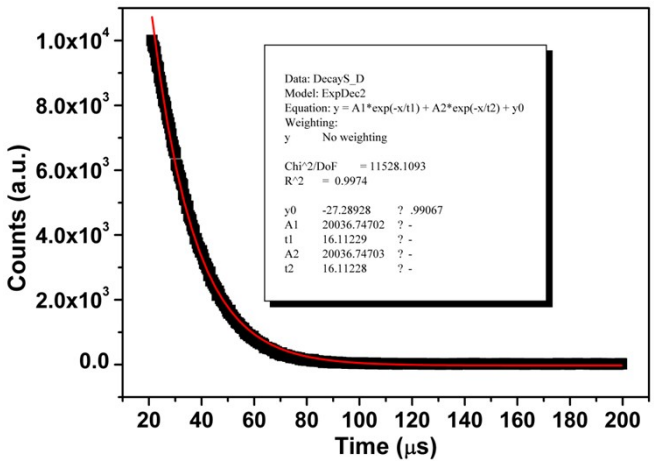

Fig. S7. Solid-state decay curve of **D-2**, fitted by a double-exponential function.

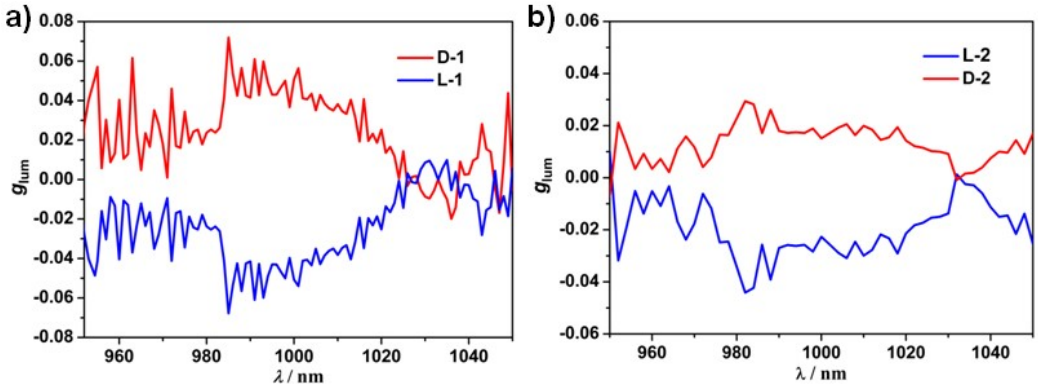

Fig. S8. Plots of g_{lum} versus wavelength for **D-1**/**L-1** (a) and **D-2**/**L-2** (b).

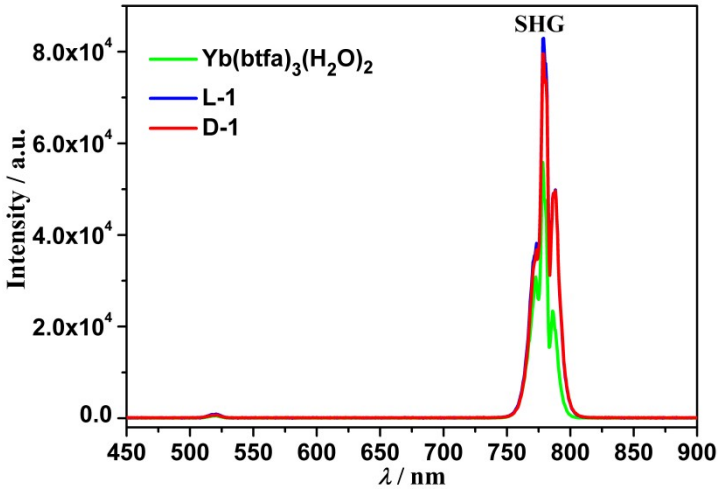

Fig. S9. SHG spectra of **D-1**/**L-1** and $Yb(btfa)_3(H_2O)_2$ under excitation at λ = 1550 nm (T_{int} = 0.5 s) at room temperature.

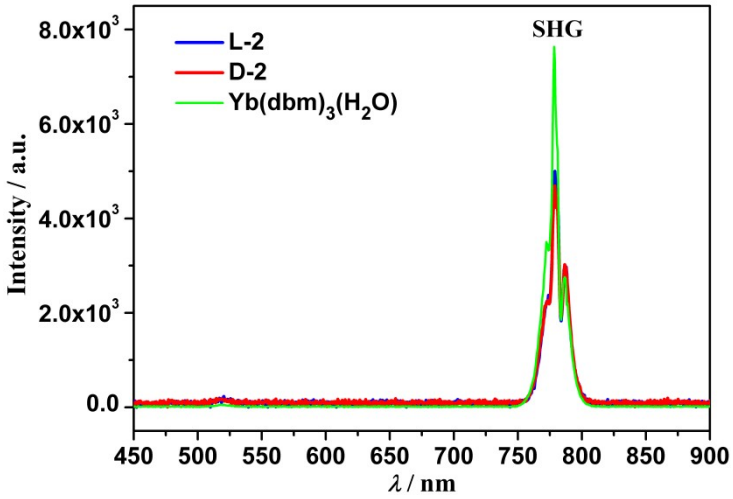

Fig. S10. SHG spectra of **D-2**/**L-2** and $Yb(dbm)_3(H_2O)$ under excitation at λ = 1550 nm (T_{int} = 0.5 s) at room temperature.

Table S1. Crystallographic data and structure refinement parameters for **D-1**/**L-1** and **D-2**/**L-2** enantiomeric pairs.

Complexes	**D-1**	**L-1**	**D-2**	**L-2**
Chemical formula	$C_{46}H_{35}F_9N_3O_6Yb$	$C_{46}H_{35}F_9N_3O_6Yb$	$C_{108}H_{89}N_3O_{13}Yb_2$	$C_{108}H_{89}N_3O_{13}Yb_2$
Formula weight	1069.81	1069.81	1982.90	1982.90
Crystal system	monoclinic	monoclinic	monoclinic	monoclinic
Space group	$P2_1$	$P2_1$	$P2_1$	$P2_1$
a (Å)	10.1341(9)	10.1213(6)	10.3289(6)	10.3498(7)
b (Å)	19.8579(13)	19.8331(10)	20.9947(12)	21.0293(11)
c (Å)	11.3131(8)	11.3132(8)	21.4061(12)	21.4472(14)
$\alpha = \gamma$ (deg)	90	90	90	90
β (deg)	95.212(7)	95.262(6)	98.852(6)	98.962(6)
V (Å^3)	2267.3(3)	2261.4(2)	4586.7(5)	4611.0(5)
Z	2	2	2	2
D_c (g cm^{-3})	1.567	1.571	1.436	1.428
μ (mm^{-1})	2.150	2.155	2.092	2.081
F(000)	1062	1062	2004	2004
Reflections collected	10216	19253	19918	21763
Independent reflections	6678	9890	14260	15146
Data/restraints/parameters	6678/1/588	9890/971/588	14260/2/1142	15146/2/1142
GOF	0.982	1.035	0.999	0.928
R_1[I > = 2σ(I)][a]	0.0468	0.0660	0.0543	0.0572
wR_2[I > = 2σ(I)][b]	0.0625	0.1300	0.0828	0.0782
Flack parameter	0.017(9)	0.026(15)	0.017(8)	0.015(7)
CCDC	2290257	2290258	2290259	2290260

[a]$R_1 = \sum||Fo|-|Fc||/\sum|Fo|$. [b]w$R_2 = [\sum w(Fo^2 - Fc^2)^2/\sum w(Fo^2)^2]^{1/2}$

Table S2. Selected bond lengths (Å) and angles (°) for **D-1** and **L-1**.

Bond lengths for **D-1**					
Yb(1)─O(1)	2.255(10)	Yb(1)─O(2)	2.262(7)	Yb(1)─O(3)	2.277(6)
Yb(1)─O(4)	2.260(7)	Yb(1)─O(5)	2.276(9)	Yb(1)─O(6)	2.295(7)
Yb(1)─N(1)	2.489(8)	Yb(1)─N(2)	2.531(7)		
Bond lengths for **L-1**					
Yb(1)─O(1)	2.273(9)	Yb(1)─O(2)	2.313(12)	Yb(1)─O(3)	2.291(9)
Yb(1)─O(4)	2.282(8)	Yb(1)─O(5)	2.286(10)	Yb(1)─O(6)	2.275(11)
Yb(1)─N(1)	2.476(10)	Yb(1)─N(2)	2.532(10)		
Bond angles for **D-1**					
O(3)-Yb(1)-O(2)	139.0(3)	O(3)-Yb(1)-O(5)	79.4(4)	O(6)-Yb(1)-O(5)	73.1(3)
O(1)-Yb(1)-O(3)	76.8(4)	O(6)-Yb(1)-N(1)	80.0(3)	O(3)-Yb(1)-N(2)	78.7(2)
Bond angles for **L-1**					
O(3)-Yb(1)-O(2)	78.7(5)	O(3)-Yb(1)-O(5)	139.1(4)	O(6)-Yb(1)-O(5)	72.6(4)
O(1)-Yb(1)-O(3)	122.1(4)	O(6)-Yb(1)-N(1)	103.1(4)	O(3)-Yb(1)-N(2)	77.9(3)

Table S3. Selected bond lengths (Å) and angles (°) for **D-2** and **L-2**.

Bond lengths for **D-2**					
Yb(1)─O(1)	2.278(9)	Yb(1)─O(2)	2.240(8)	Yb(1)─O(3)	2.248(8)
Yb(1)─O(4)	2.278(7)	Yb(1)─O(5)	2.267(8)	Yb(1)─O(6)	2.266(8)
Yb(1)─N(1)	2.558(9)	Yb(1)─N(2)	2.546(9)	Yb(2)─O(13)	2.359(9)
Yb(2)─O(7)	2.230(8)	Yb(2)─O(8)	2.247(9)	Yb(2)─O(9)	2.221(8)
Yb(2)─O(10)	2.258(9)	Yb(2)─O(11)	2.249(8)	Yb(2)─O(12)	2.230(9)
Bond lengths for **L-2**					
Yb(1)─O(1)	2.300(7)	Yb(1)─O(2)	2.282(7)	Yb(1)─O(3)	2.249(8)
Yb(1)─O(4)	2.293(7)	Yb(1)─O(5)	2.290(8)	Yb(1)─O(6)	2.263(8)
Yb(1)─N(1)	2.577(9)	Yb(1)─N(2)	2.531(9)	Yb(2)─O(13)	2.364(9)
Yb(2)─O(7)	2.260(8)	Yb(2)─O(8)	2.257(8)	Yb(2)─O(9)	2.253(8)
Yb(2)─O(10)	2.224(8)	Yb(2)─O(11)	2.255(8)	Yb(2)─O(12)	2.240(8)
Bond angles for **D-2**					
O(3)-Yb(1)-O(2)	115.4(3)	O(3)-Yb(1)-O(5)	79.3(3)	O(6)-Yb(1)-O(5)	75.0(3)
O(1)-Yb(1)-O(3)	73.4(3)	O(6)-Yb(1)-N(1)	115.5(3)	O(3)-Yb(1)-N(2)	135.9(3)
O(5)-Yb(1)-N(2)	103.8(3)	O(2)-Yb(1)-N(1)	134.9(3)	N(1)-Yb(1)-N(2)	62.8(3)
O(9)-Yb(2)-O(12)	150.1(3)	O(7)-Yb(2)-O(8)	75.5(3)	O(7)-Yb(2)-O(10)	106.0(3)
O(8)-Yb(2)-O(11)	90.7(3)	O(9)-Yb(2)-O(10)	75.8(3)	O(8)-Yb(2)-O(10)	154.2(3)
Bond angles for **L-2**					
O(3)-Yb(1)-O(2)	143.7(2)	O(3)-Yb(1)-O(5)	73.8(3)	O(6)-Yb(1)-O(5)	73.0(3)
O(1)-Yb(1)-O(3)	79.6(3)	O(6)-Yb(1)-N(1)	134.9(3)	O(3)-Yb(1)-N(2)	136.6(3)
O(5)-Yb(1)-N(2)	74.6(3)	O(2)-Yb(1)-N(1)	115.1(3)	N(1)-Yb(1)-N(2)	63.2(3)
O(9)-Yb(2)-O(12)	80.3(3)	O(7)-Yb(2)-O(8)	75.9(3)	O(7)-Yb(2)-O(10)	79.2(3)
O(8)-Yb(2)-O(11)	82.8(3)	O(9)-Yb(2)-O(10)	76.2(3)	O(8)-Yb(2)-O(10)	79.1(3)

Table S4. Continuous shape measures calculation for Yb1 in **D-1**.

OP-8	1 D_{8h}	Octagon
HPY-8	2 C_{7v}	Heptagonal pyramid
HBPY-8	3 D_{6h}	Hexagonal bipyramid
CU-8	4 O_h	Cube
SAPR-8	5 D_{4d}	Square antiprism
TDD-8	6 D_{2d}	Triangular dodecahedron
JGBF-8	7 D_{2d}	Johnson gyrobifastigium J26
JETBPY-8	8 D_{3h}	Johnson elongated triangular bipyramid J14
JBTPR-8	9 C_{2v}	Biaugmented trigonal prism J50
BTPR-8	10 C_{2v}	Biaugmented trigonal prism
JSD-8	11 D_{2d}	Snub diphenoid J84
TT-8	12 T_d	Triakis tetrahedron
ETBPY-8	13 D_{3h}	Elongated trigonal bipyrami

Structure [ML8]	OP-8	HPY-8	HBPY-8	CU-8	SAPR-8	TDD-8	JGBF-8	JETBPY-8	JBTPR-8	BTPR-8	JSD-8	TT-8	ETBPY-8
ABOXIY	28.888	22.973	16.427	9.791	**0.652**	1.639	15.122	27.158	2.172	1.638	4.221	10.467	23.489

Table S5. Continuous shape measures calculation for Yb1 in **D-2**.

OP-8	1 D_{8h}	Octagon
HPY-8	2 C_{7v}	Heptagonal pyramid
HBPY-8	3 D_{6h}	Hexagonal bipyramid
CU-8	4 O_h	Cube
SAPR-8	5 D_{4d}	Square antiprism
TDD-8	6 D_{2d}	Triangular dodecahedron
JGBF-8	7 D_{2d}	Johnson gyrobifastigium J26
JETBPY-8	8 D_{3h}	Johnson elongated triangular bipyramid J14
JBTPR-8	9 C_{2v}	Biaugmented trigonal prism J50
BTPR-8	10 C_{2v}	Biaugmented trigonal prism
JSD-8	11 D_{2d}	Snub diphenoid J84
TT-8	12 T_d	Triakis tetrahedron
ETBPY-8	13 D_{3h}	Elongated trigonal bipyrami

Structure [ML8]	OP-8	HPY-8	HBPY-8	CU-8	SAPR-8	TDD-8	JGBF-8	JETBPY-8	JBTPR-8	BTPR-8	JSD-8	TT-8	ETBPY-8
ABOXIY	29.472	23.267	15.925	10.470	**0.606**	2.040	14.932	26.907	2.394	1.933	4.385	11.221	23.388

Table S6. Continuous shape measures calculation for Yb2 in **D-2**.

HP-7	1 D_{7h}	Heptagon
HPY-7	2 C_{6v}	Hexagonal pyramid
PBPY-7	3 D_{5h}	Pentagonal bipyramid
COC-7	4 C_{3v}	Capped octahedron
CTPR-7	5 C_{2v}	Capped trigonal prism
JPBPY-7	6 D_{5h}	Johnson pentagonal bipyramid J13
JETPY-7	7 C_{3v}	Johnson elongated triangular pyramid J7

Structure [ML7]	HP-7	HPY-7	PBPY-7	COC-7	CTPR-7	JPBPY-7	JETPY-7
ABOXIY	35.069	19.607	7.231	**0.514**	1.060	10.831	18.518

Table S7. Calculated dipole moments of **D-1** and **D-2**.

Compound	**D-1**	**D-2**
μ_{total} (D)	7.1437	2.7289
X	–4.0079	–0.1079
Y	2.0216	1.9393
Z	5.5198	–1.9169